NACA RM E56K28b

NACA

RESEARCH MEMORANDUM

AN INLET DESIGN CONCEPT TO REDUCE FLOW DISTORTION AT ANGLE OF ATTACK

By Carl F. Schueller and Leonard E. Stitt

Lewis Flight Propulsion Laboratory
Cleveland, Ohio

NATIONAL ADVISORY COMMITTEE
FOR AERONAUTICS

WASHINGTON

February 26, 1957
Declassified December 3, 1958

NATIONAL ADVISORY COMMITTEE FOR AERONAUTICS

RESEARCH MEMORANDUM

AN INLET DESIGN CONCEPT TO REDUCE FLOW DISTORTION AT ANGLE OF ATTACK

By Carl F. Schueller and Leonard E. Stitt

SUMMARY

Detailed pressure measurements were made of the flow distortion just inside the cowl lip of a fixed-cone planar-cowl inlet, a pivoting-cone planar-cowl inlet and a pivoting-cone swept-cowl inlet operated at angles of attack from 0° to 14° and at a Mach number of 1.91. The overall pressure recovery and flow distortion at the exit of the three diffusers were also measured.

Considerable flow distortion occurred on the inside of the bottom lip of a planar cowl operated at angle of attack. This appeared to result from the high turning angle required of the subsonic filament of air which was outside the cone oblique shock but captured by the inlet. Sweeping the cowl lip back, from top to bottom, maintained the cone oblique shock ahead of the bottom lip at angle of attack. This resulted in preturning of the air ahead of the lip, and lower distortions and higher pressure recoveries were obtained.

INTRODUCTION

Inlet-flow distortion is now recognized as an important problem because of the results of various investigations (e.g., refs. 1 to 4), which have demonstrated the associated adverse effects on turbojet engine performance. Although the magnitude of flow distortion will vary from inlet to inlet, all axisymmetric spike-type inlets have encountered increasing distortion when operated at high angles of attack. Several attempts (refs. 5 to 7) were made to design nose inlets which had improved pressure recovery and mass-flow characteristics at angle of attack. Also studies (refs. 8 and 9) to improve the distortion were made using screens and flow-straightening devices in the subsonic portion of the diffuser. All these investigations had only limited success in improving distortion as a result of ineffectiveness at high angles of attack or of built-in performance penalties when the inlets were operated at the cruise condition.

The present study is concerned with the origin of flow distortion at the lips of supersonic inlets operating at angle of attack. Detailed total-pressure surveys at the throat of three axisymmetric supersonic inlets operating at a Mach number of 1.91 and angles of attack from 0° to 14° were used in the present investigation.

QUALITATIVE ANALYSIS

By considering only the effect of angle of attack on distortion and inlet performance, it has been pointed out many times that as the angle of attack is increased, the lee side of the cone contributes a decreasing amount of compression and eventually flow separation occurs. Thus, the air enters the inlet with considerable distortion. Use of a pivoted cone, as in reference 7, should eliminate this source of trouble. However, analysis of unpublished data for the pivoted cone model shows that prohibitive distortions still exist at a 14° angle of attack for the shock on lip configurations. An examination of the theoretical shock configuration indicated that as the angle of attack was increased, the oblique shock from the spike fell inside the cowl lip at the bottom quadrant. This required the air entering the bottom of the cowl to expand around the cowl lip approximately 26° more than required at a zero angle of attack. Accordingly, in designing the modified inlet reported herein, it was reasoned that the bottom of the cowl was experiencing flow separation that was as important a source of trouble as the lee side of the spike. It was further proposed that the area of trouble be alleviated by sweeping back the cowl so that the bottom lip was aft of the top lip and always behind the cone oblique shock. The sweep is geometrically similar to that used on normal-shock inlets in the past (e.g., refs. 10 to 12); however, the purpose of the sweep in this case was to maintain the oblique shock ahead of the bottom cowl lip and thus provide preturning equal to the turning in the flow field of the compression surface. Techniques other than sweep, for example, centerbody translation, could be used to satisfy the concept of preturning.

SYMBOLS

A	flow area
l	subsonic diffuser length
M	Mach number
m	mass flow
P	total pressure

X lineal distance

α angle of attack

θ_l angle between cone tip and cowl lip and axis of model

Subscripts:

av average

max maximum

min minimum

x condition at x-distance

0 free stream

1 inlet rake station

2 diffuser-exit rake station

APPARATUS AND PROCEDURE

The model of reference 7 (see fig. 1) was rerun with two total-pressure rakes installed near the inlet throat at the top and bottom of the passage. A survey of the entering flow was obtained for this model, with and without cone pivoting over a range of angle of attack with the cone positioned for shock on the lip at zero angle of attack, or at a cowl-lip parameter θ_l of 44°. Flow distortion at the end of the diffuser was also measured for shock ahead of the lip when θ_l was 41.8°.

The forward 15 percent of this model was then modified by (1) sweeping back the cowl lip 14° from top to bottom, and (2) moving the effective center of rotation of the 25° half-angle cone aft, so that the cone shoulder would not be ahead of the lower inlet lip. The internal lip angle varied from 10.2° at the top of the cowl to 7.7° at the bottom as compared with 12° for the inlet of reference 7. The instrumentation that was used to obtain the inlet profiles and diffuser-exit conditions presented herein is shown in figure 1. A comparison of the internal area variation of the two models is shown in figure 2.

Inlet mass flow was computed from a measured static pressure behind the exit rake station and a choked plug, assuming no total-pressure loss between the two stations. The theoretical capture mass flow of all inlets was based on the reference area at zero angle of attack.

For the swept-cowl inlet, the reference mass flow used in the mass-flow ratio was a circular area defined by the radius of the upper inlet lip. This would correspond to the projected area of a similar inlet with an unswept cowl.

The diffuser-exit total-pressure recovery was computed from the reference mass flow and a measured static pressure at the exit rake station.

At each angle of attack, the cone was alined with the stream by means of replaceable wedges at the base of the cone. A photograph of the model is shown in figure 3. The model angle of attack was varied by means of the support strut and was limited to 14° because of model and tunnel size. Stability limits were determined by visual observation of the shadowgraph.

The investigation was conducted in the Lewis 18- by 18-inch supersonic wind tunnel at a Mach number of 1.91 and a Reynolds number of 3.1×10^6 per foot.

RESULTS AND DISCUSSION

The reasons for expecting considerable distortion of the internal flow to originate at the bottom of inlets designed for shock on lip at zero angle of attack but operated at 14° angle of attack are shown schematically in figure 4. The theoretical shock and turning angles at the bottom of three different axisymmetric inlet configurations are shown for critical inlet operation. It is noted that the subsonic filament of air (see figs. 4(a) and (b)), which is outside the oblique shock but captured by the inlet, has no prior turning. This subsonic flow must either turn abruptly through 26° to follow the inside of the cowl or separate. Sweeping the cowl lip back so that the bottom is always behind the oblique shock, as shown in figure 4(c), results in preturning the air ahead of the lip (approximately 12° according to cone flow charts) and reduces the turning angle from 21.7° to 9.70° for this particular cowl design.

The preceding concept was confirmed by the inlet total-pressure profiles shown in figure 5 for the three inlet configurations operating at 0° to 14° angles of attack for both critical and 5 to 8 percentage points subcritical inlet mass-flow ratios. For example, at critical inlet conditions and a 14° angle of attack (fig. 5(d)), inlet recoveries of approximately 97 percent are measured at the bottom of the swept cowl. For the straight cowl, however, pressure recoveries of 75 percent for the fixed-cone configuration and 50 percent for the pivoted cone are indicated at the bottom lip. Actually, flow separation is indicated for the straight-cowl pivoted-cone model since the total-pressure recovery

of 50 percent equals the local static pressure. It is also considerably less than the 77 percent recovery, which should be obtained for a filament of air passing through a normal shock at Mach number 1.91. The improved pressure recovery near the bottom cowl lip for the fixed cone (75 percent) compared with the pivoted cone (50 percent) is in contradiction with the flow hypothesized in figure 4. The shadowgraph pictures presented in figure 6 provide a qualitative explanation of the difference. A comparison of the shock formation at the bottom of the cowls shows that a strong oblique shock is formed with the cone-fixed configuration rather than the normal shock formed with the pivoted-cone inlet. The strong oblique shock probably introduces some turning ahead of the lip and should reduce the pressure loss across the shock, thus increasing the local recovery from 50 to 75 percent. This value is still considerably less than the 97 percent obtained with the swept cowl.

The results of applying the concept of moderate turning angles at the bottom of a cowl are shown in figure 7, as the variation with mass-flow ratio of inlet-flow distortion and pressure recovery for angles of attack from 0° to 14°. The straight-cowl fixed-cone configuration had the greatest decrease in performance. The critical total-pressure recovery decreased from 88 to 69 percent, and the distortion increased from 4 to 23 percent as the angle of attack increased from 0° to 14°. Using the straight cowl and pivoting the cone did not significantly improve the distortion at the diffuser exit. However, with the swept-cowl pivoted-cone configuration, the distortion increased only from 9 to 14 percent while the pressure recovery decreased from 87 to 84 percent up to 14° angle of attack. Thus, the swept cowl serves a very useful function in reducing the rate of increase of flow distortion with angle of attack; however, for the inlet used in this study the distortion at zero angle of attack was 9 percent for the swept cowl as compared with 4 percent for the straight cowl. Based on the variation of the total-pressure recovery in the inlet-flow annulus, which is shown in figure 5(a), the increased distortion for the swept cowl is originating on the bottom of the centerbody as indicated by the low total-pressure recovery which extends over 20 percent of the annulus height. The reason the separation is aggravated by the swept cowl is not known, but differences in internal geometry may be contributing factors. In any case, centerbody throat bleed might be very beneficial. The preceding discussion was related to critical inlet operation as a matter of convenience. However, application of an inlet to an engine would generally result in operation at subcritical mass-flow ratios (constant corrected airflow) with an increasing angle of attack. For the data reported in figure 7, this application would result in lower absolute values of distortion, but the advantages of preturning would still exist.

Contours of the total-pressure distribution at the exit of the subsonic diffuser for the three inlet configurations investigated are presented in figure 8 for 0° and 14° angles of attack. These contours correspond to the inlet conditions presented in figure 5. In general, regions of low-energy air, which were measured at the inlet face, persist to the diffuser exit. The very adverse effect of centerbody separation on the level of distortion at a zero angle of attack for the swept-cowl pivoted-cone configuration is apparent from figure 8(a). Also the spreading of the low-energy air, which originates at the bottom of the straight-cowl lip configurations at a 14° angle of attack, is obvious from figure 8(b).

The concept of maintaining preturning of the air ahead of the bottom lip for inlets operating at positive angles of attack should also be satisfied by translating the compression surface forward, relative to the cowl lip. Comparison of unpublished distortion data when the cone is forward so that the oblique shock is approximately 2.2° ahead of the cowl lip at zero angle of attack with data for the shock slightly inside the lip is presented in figure 9 as the variation of diffuser-exit distortion at critical inlet operation with angle of attack. Although the determination of the critical inlet condition is subject to question for inlets operating at angle of attack, the limited data of figure 9 do show that for the shock-inside-the-lip configuration (θ_l, 44.7°) the distortion starts to increase at angles of attack as low as 3°. For the configuration with the shock 2.2° ahead of the lip (θ_l, 41.8°), the distortion was less over the angle-of-attack range.

With a θ_l of 41.8°, the oblique shock would remain ahead of the cowl up to an angle of attack of about 10°. However, the distortion begins to increase rapidly at some angle of attack between 3° and 8°, and at 10° is greater than with the swept cowling. This may have been a result of the additional 4° turning required at the bottom of the unswept cowl as compared with the swept cowl (7.7° as compared with 12°, fig. 1).

The preceding discussion has demonstrated the principles of preturning the air ahead of the bottom cowl lip for angle-of-attack operation by maintaining the compression-surface oblique shock ahead of the bottom lip. In addition to the applications studied in this investigation, a number of alternative configurations are as follows:

(a) Mount the centerbody eccentrically and reduce the spillage drag at zero angle of attack.

(b) Reduce the spillage drag at zero angle of attack by substituting for the planar sweep of the cowl lip a cowling cut which corresponds to the intersection of the cone oblique shock with the cowling at the highest angle of attack desired.

(c) Design the centerbody with a higher cone angle at the bottom than at the top. With a properly positioned planar cowl air would be spilled at zero angle of attack, but the oblique shock would be ahead of the bottom section of the cowl lip at angle of attack.

The techniques which are used for the nacelle installation should also be applicable to side-inlet installations. However, the application may be more specific for each configuration since the local flow angles at the cowl lip will be influenced by such things as the type of side inlet used, the fuselage shape, and, possibly, the canopy flow field.

CONCLUSIONS

Based on the preliminary experiments reported herein for conical centerbody-type supersonic inlets, the following conclusions are obtained:

1. At critical or subcritical mass-flow ratios, considerable flow distortion and pressure-recovery losses corresponding to flow separation can occur at the bottom of planar cowls when they are operated at angle of attack. These adverse flow conditions result from the excessive turning required of the subsonic filament of air which is outside the cone oblique shock and has no prior turning but is captured by the inlet.

2. Positioning the oblique shock ahead of the bottom of the cowl lip for angle-of-attack operation, for example by sweeping the cowl, reduces the required turning at the cowl lip by the amount of turning obtained with the compression surface. As a result, in going from a 0° to a 14° angle of attack the distortion at critical inlet flow increased from 9 to only 14 percent as compared with 4 to 23 percent for a planar cowl. Correspondingly, the critical pressure recovery decreased from 87 to 84 percent for the swept cowl and from 88 to 69 percent for the planar cowl.

3. Pivoting the cone did not appear to be a major factor in reducing flow distortion at the diffuser exit for the higher angles of attack.

4. Translating the centerbody so that the oblique shock was ahead of the planar cowl at zero angle of attack also provided preturning and thus reduced the distortion at the higher angles of attack.

Lewis Flight Propulsion Laboratory
National Advisory Committee for Aeronautics
Cleveland, Ohio, November 27, 1956

REFERENCES

1. Conrad, E. William, Hanson, Morgan P., and McAulay, John E.: Effects of Inlet-Air-Flow Distortion on Steady-State Altitude Performance of an Axial-Flow Turbojet Engine. NACA RM E55A04, 1955.

2. Smith, Ivan D., Braithwaite, W. M., and Calvert, Howard F.: Effect of Inlet-Air-Flow Distortions on Steady-State Performance of J65-B-3 Turbojet Engine. NACA RM E55I09, 1956.

3. Harry, David P., III, and Lubick, Robert J.: Inlet-Air Distortion Effects of Stall, Surge, and Acceleration Margin of a Turbojet Engine Equipped with Variable Compressor Inlet Guide Vanes. NACA RM E54K26, 1955.

4. Fenn, David B., and Sivo, Joseph N.: Effect of Inlet Flow Distortion on Compressor Stall and Acceleration Characteristics of a J65-B-3 Turbojet Engine. NACA RM E55F20, 1955.

5. Leissler, L. Abbott, and Hearth, Donald P.: Preliminary Investigation of Effect of Angle of Attack on Pressure Recovery and Stability Characteristics for a Vertical-Wedge-Nose Inlet at Mach Number of 1.90. NACA RM E52E14, 1952.

6. Beheim, Milton A.: A Preliminary Investigation at Mach Number 1.91 of an Inlet Configuration Designed for Insensitivity to Positive Angle-of-Attack Operation. NACA RM E53E20, 1953.

7. Beheim, Milton A.: A Preliminary Investigation at Mach Number 1.91 of a Diffuser Employing a Pivoted Cone to Improve Operation at Angle of Attack. NACA RM E53I30, 1953.

8. Piercy, Thomas G., and Klann, John L.: Experimental Investigation of Methods of Improving Diffuser-Exit Total-Pressure Profiles for a Side-Inlet Model at Mach Number 3.05. NACA RM E55F24, 1955.

9. Johnston, I. H.: The Use of Freely Rotating Blade Rows to Improve Velocity Distributions in an Annulus. Memo. No. M.109, British N.G.T.E., Feb. 1951.

10. Dennard, John S., and Nelson, William J.: Preliminary Investigation of the Effects of Inlet Asymmetry on the Performance of Converging-Diverging Diffusers at Transonic Speeds. NACA RM L52J20, 1952.

11. Carter, Howard S., and Merlet, Charles F.: Preliminary Investigation of the Total-Pressure-Recovery Characteristics of a Symmetric and an Asymmetric Nose Inlet over a Wide Range of Angle of Attack at Supersonic Mach Numbers. NACA RM L53J30, 1953.

12. Dickie, George D., Jr.: Theoretical and Experimental Pressure Recovery of Sweptback Normal Shock Inlets. Jour. Aero. Sci., vol. 22, no. 3, Mar. 1955, pp. 189-193.

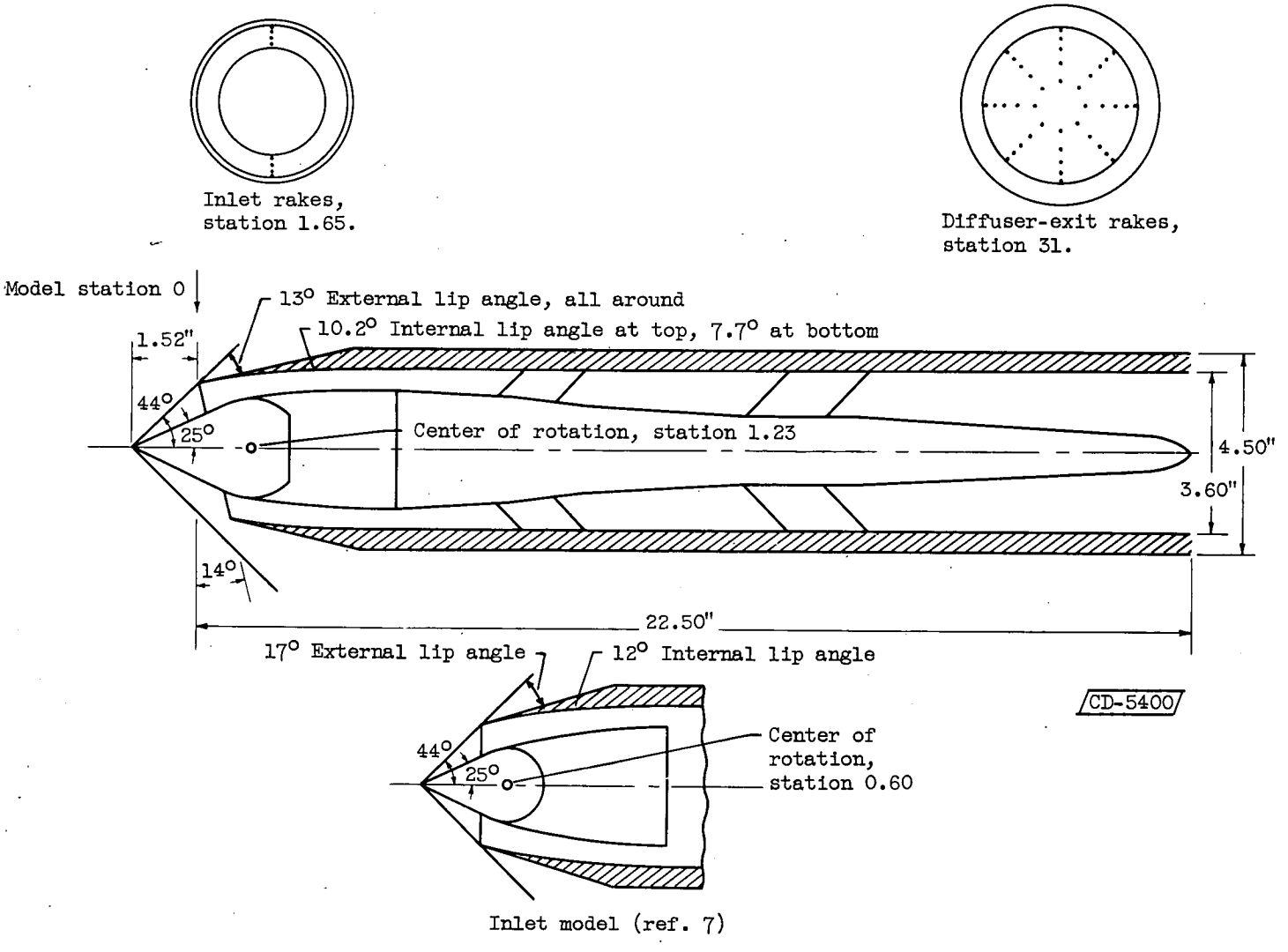


Figure 1. - General arrangements and principal dimensions of inlets.

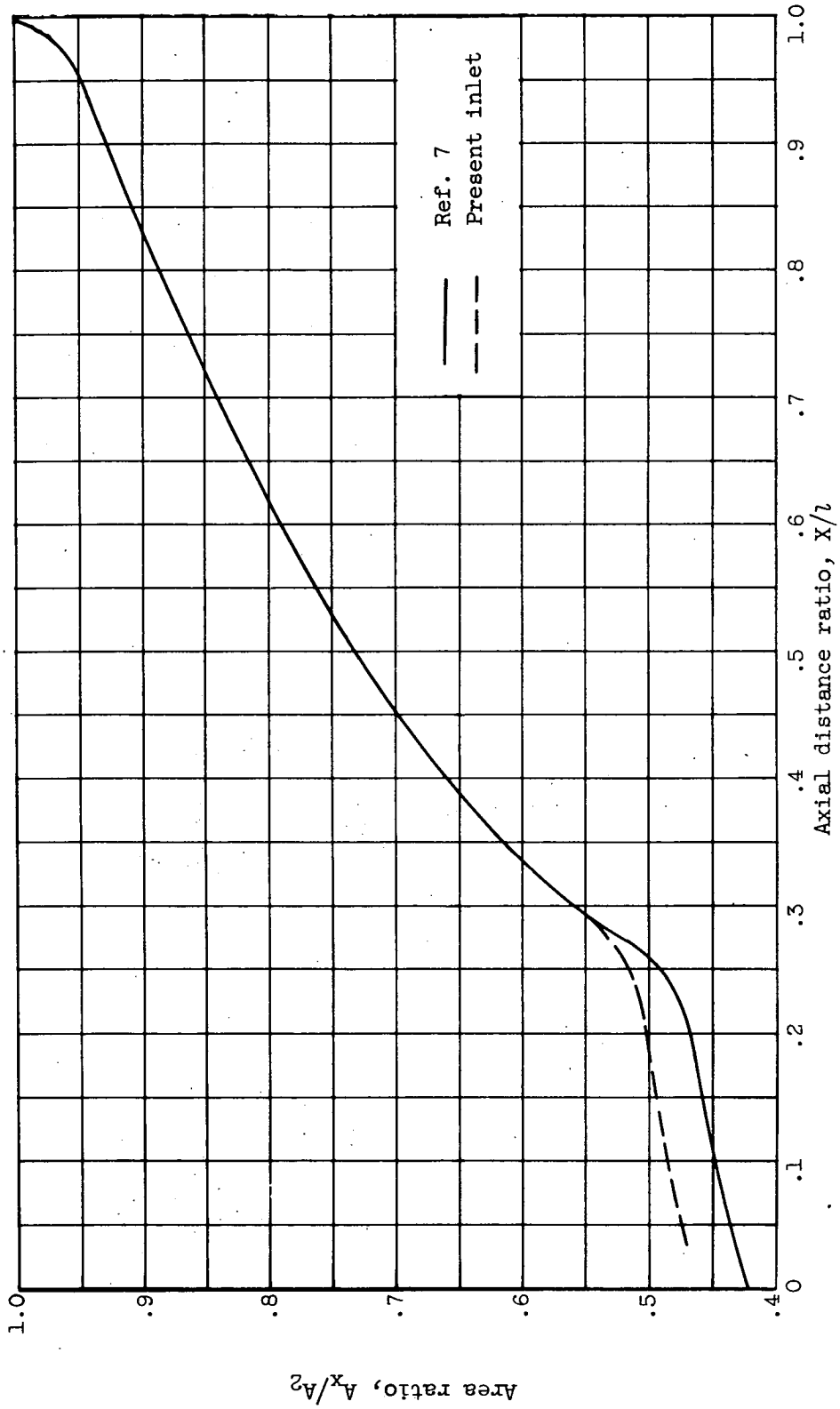
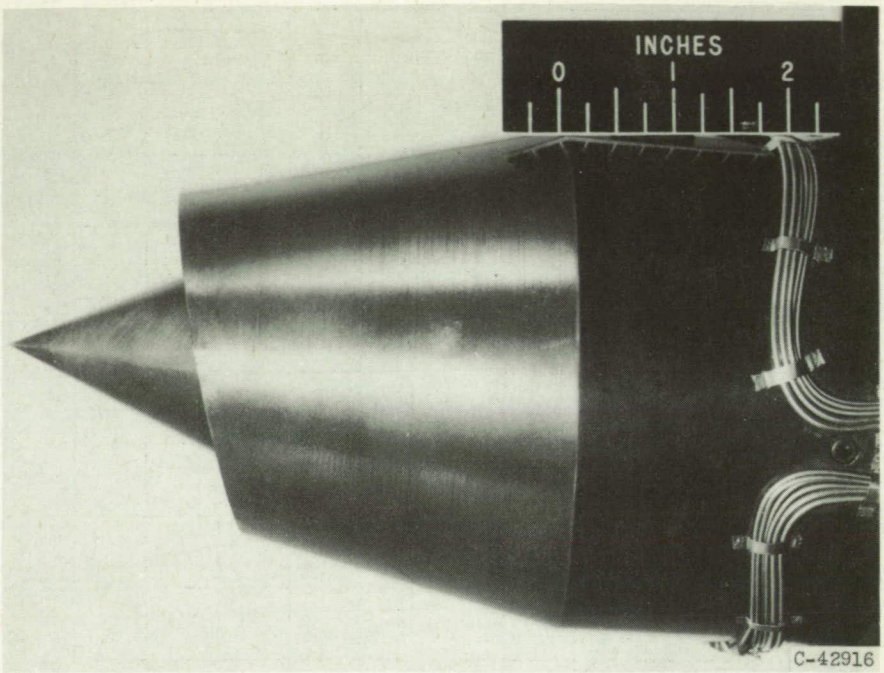
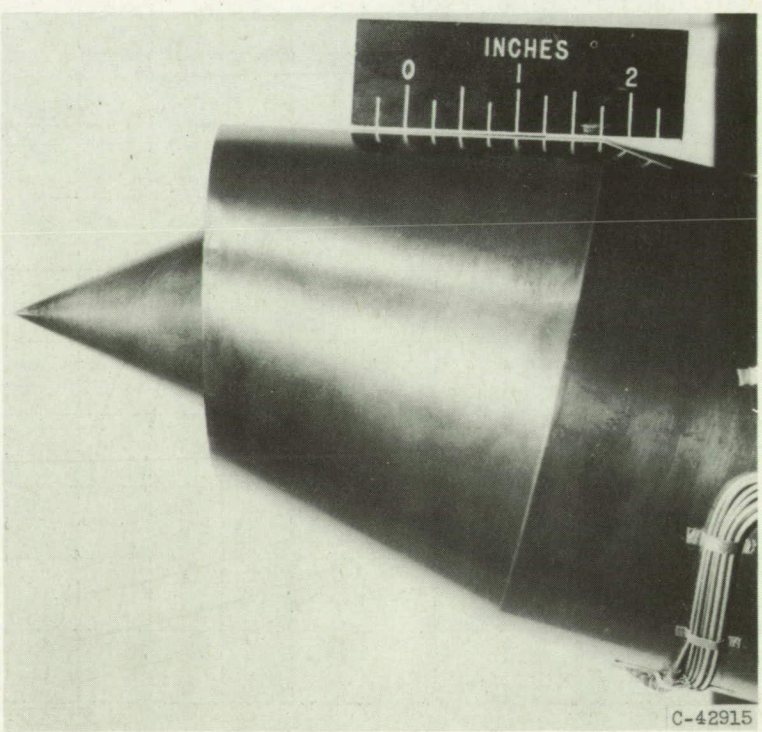


Figure 2. - Internal-area variation. Length of diffuser, 22.5 inches; diffuser-exit area, 10.18 square inches.

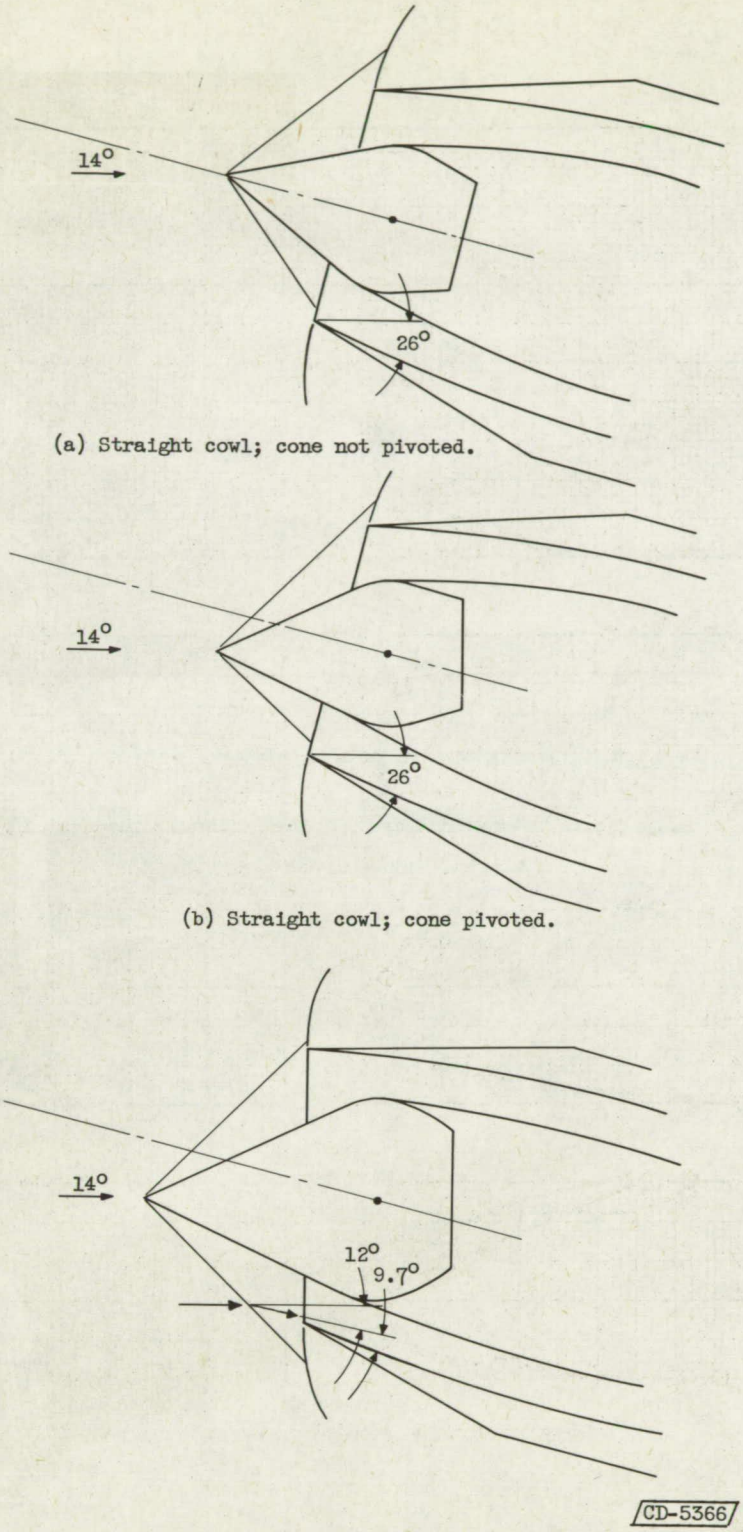


(a) Angle of attack, 0°.



(b) Angle of attack, 14°.

Figure 3. - Side view of model in tunnel.



(a) Straight cowl; cone not pivoted.

(b) Straight cowl; cone pivoted.

(c) Swept cowl; cone pivoted.

Figure 4. - Representative flow conditions at bottom of inlets. Angle of attack, 14°; free-stream Mach number, 1.91.

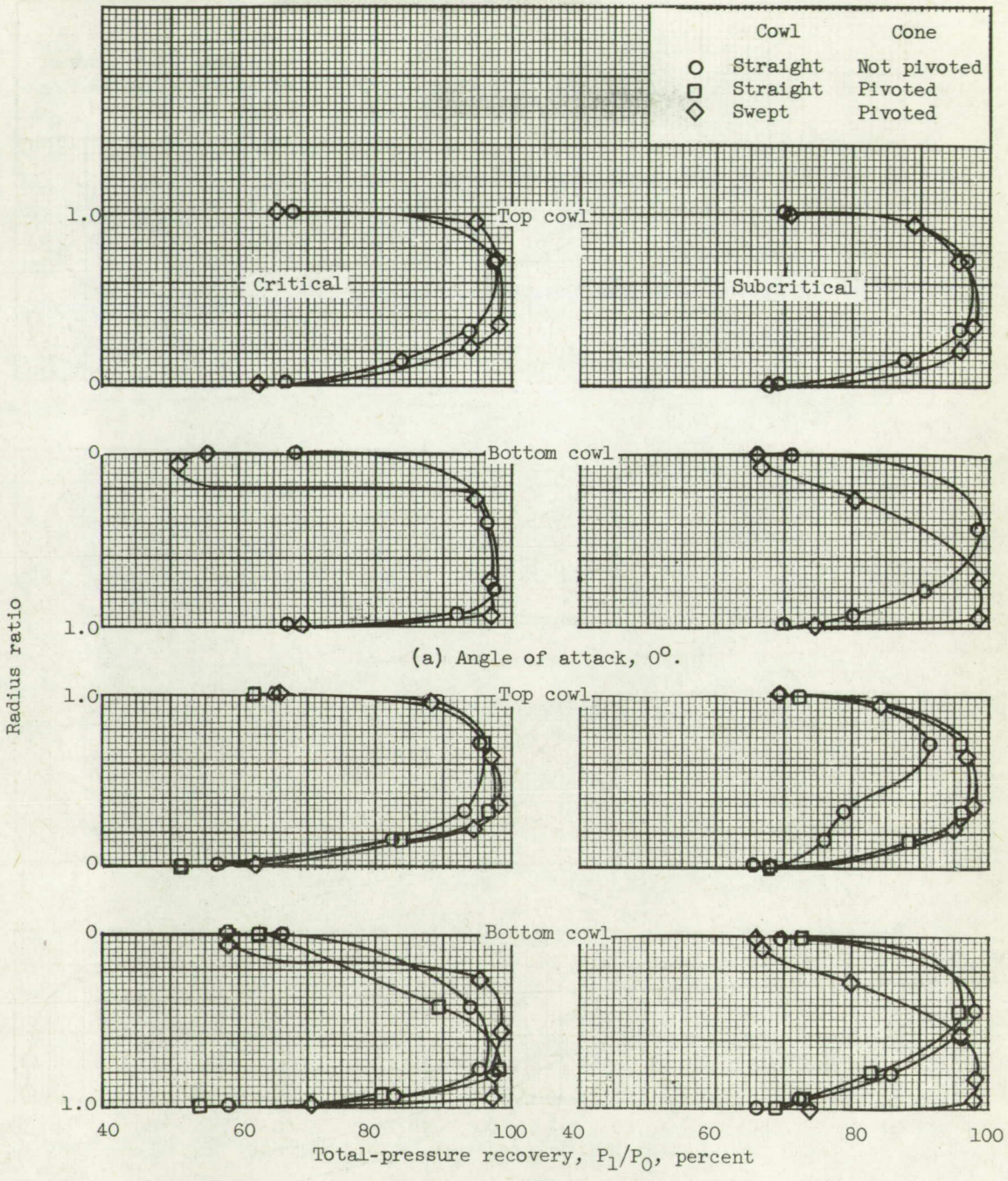
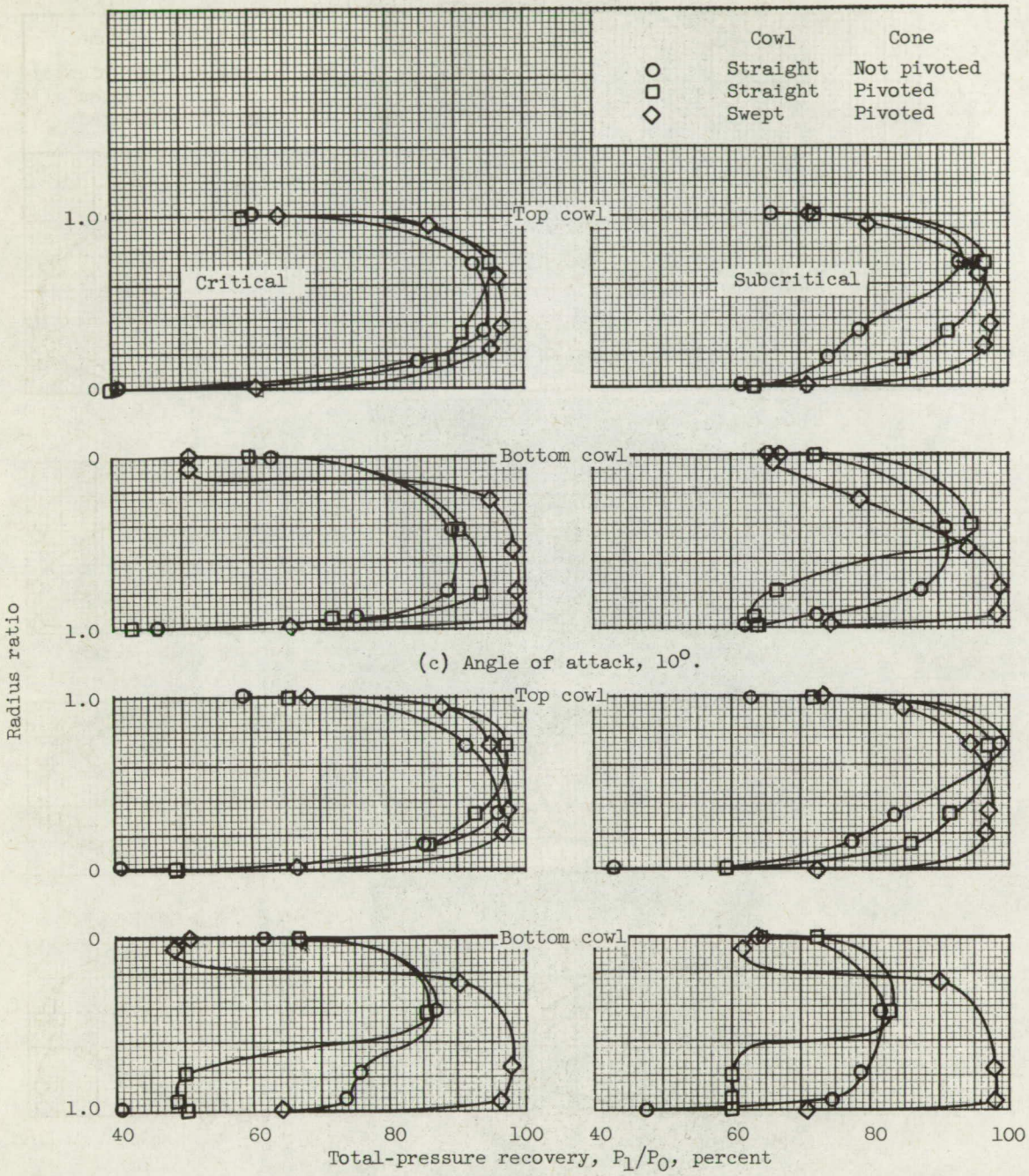


Figure 5. - Total-pressure-recovery profiles at inlet station 1.65.



(c) Angle of attack, 10°.

(d) Angle of attack, 14°.

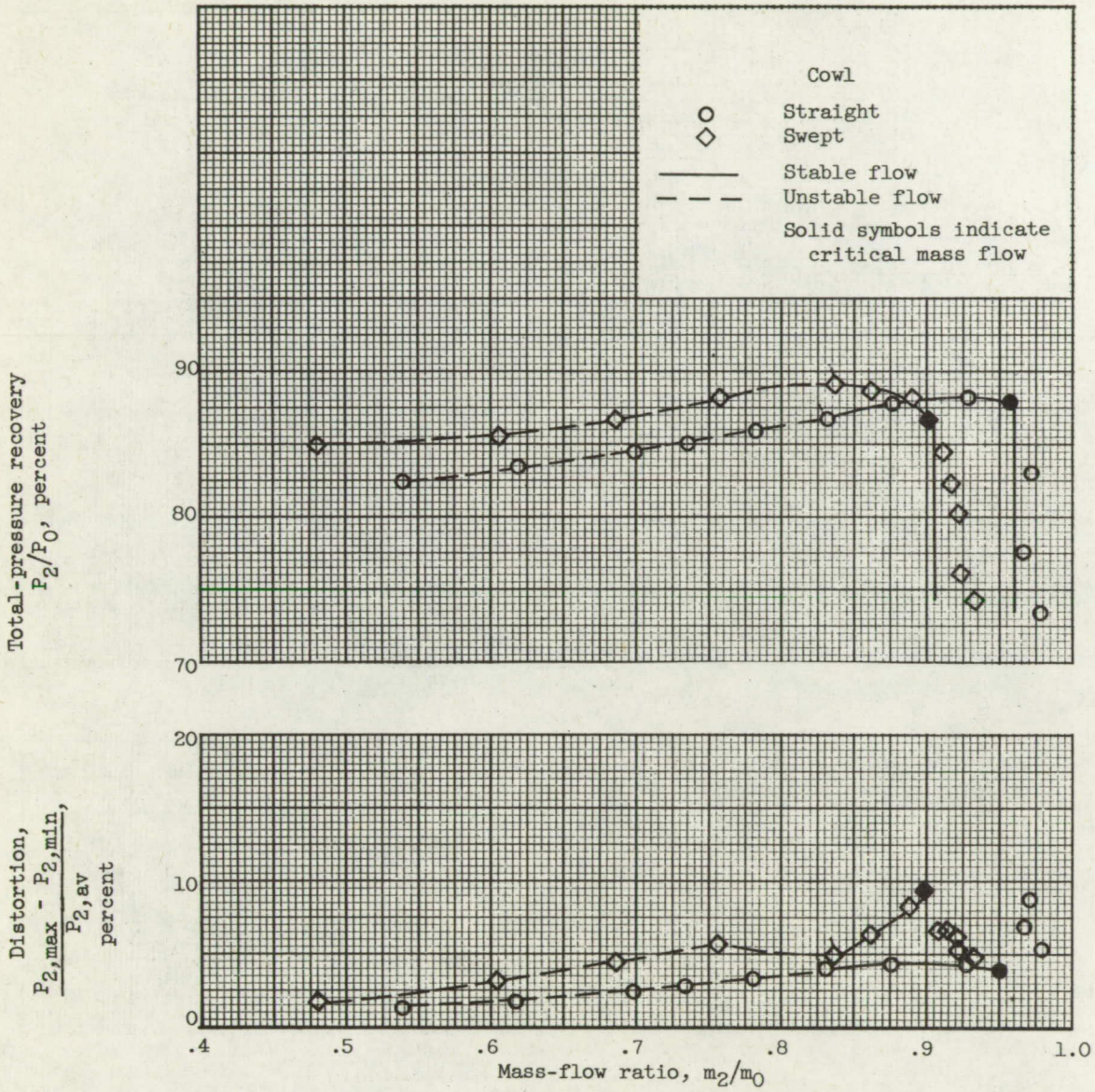
Figure 5. - Concluded. Total-pressure-recovery profiles at inlet station 1.65.

(a) Straight cowl; cone not pivoted; total-pressure recovery, 0.853; mass-flow ratio, 0.688.

(b) Straight cowl; cone pivoted; total-pressure recovery, 0.847; mass-flow ratio, 0.741.

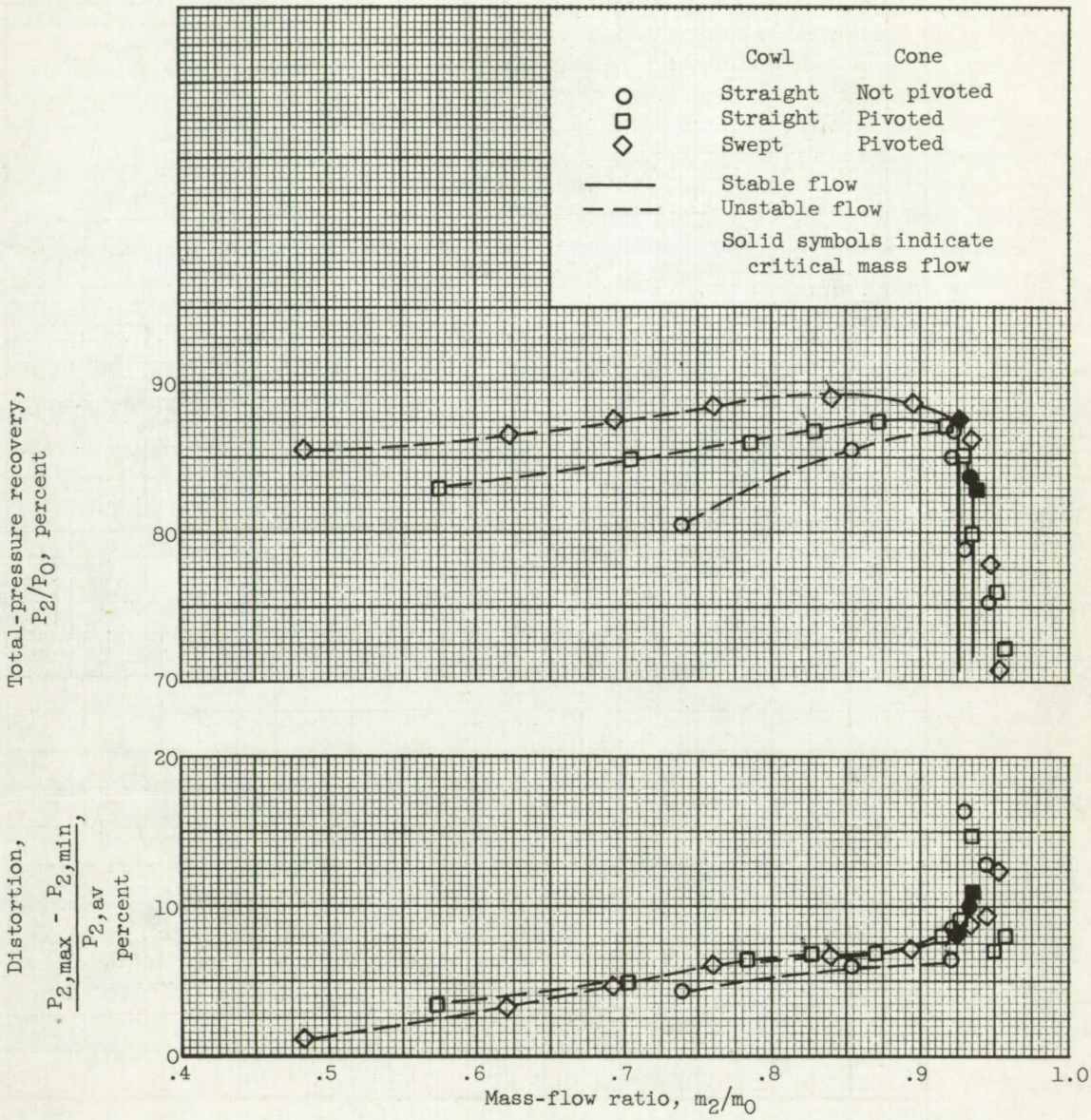
(c) Swept cowl; cone pivoted; total-pressure recovery, 0.877; mass-flow ratio, 0.840.

Figure 6. - Inlet shock structure. Angle of attack, 14°.



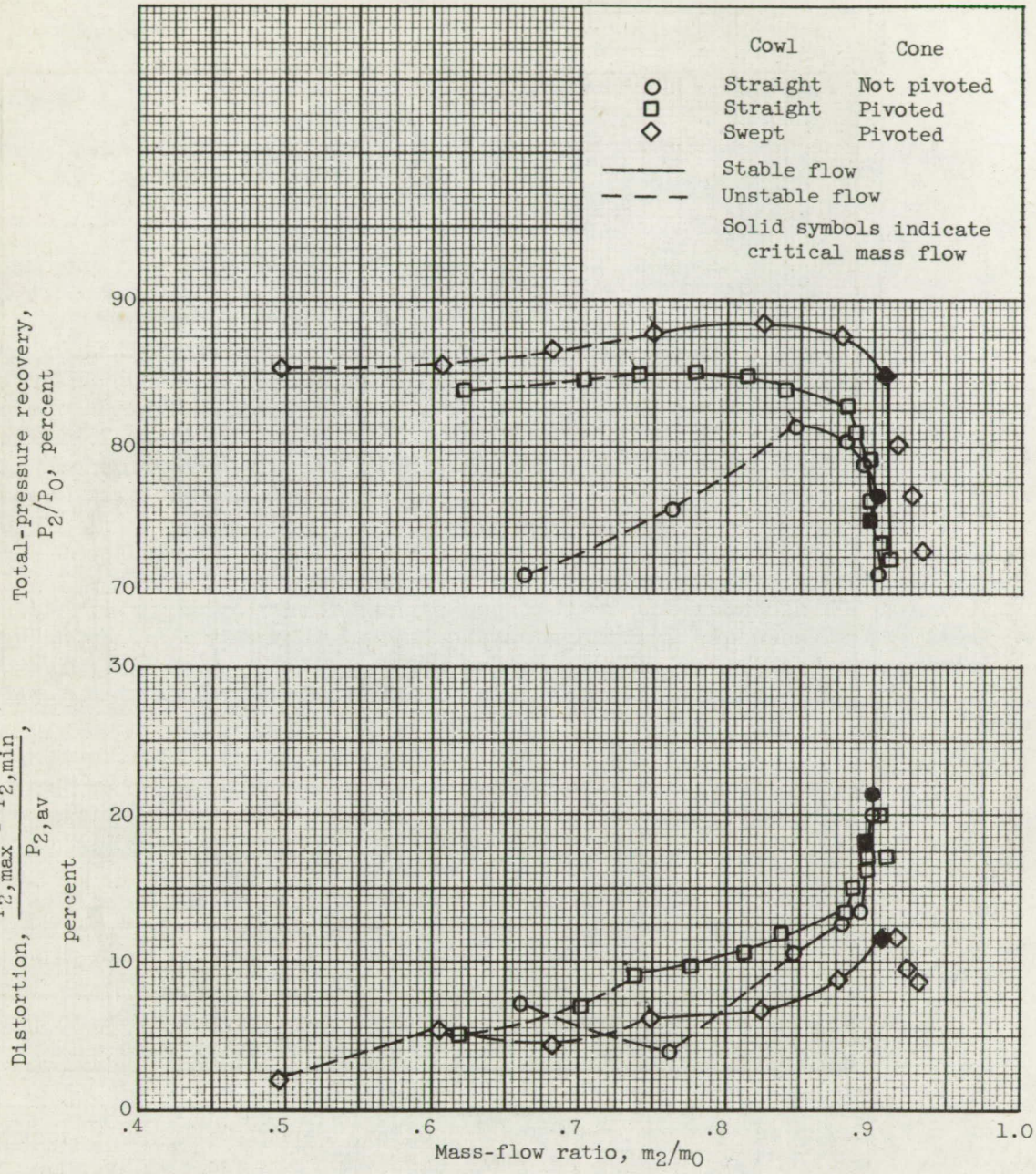
(a) Angle of attack, 0°.

Figure 7. - Performance curves.



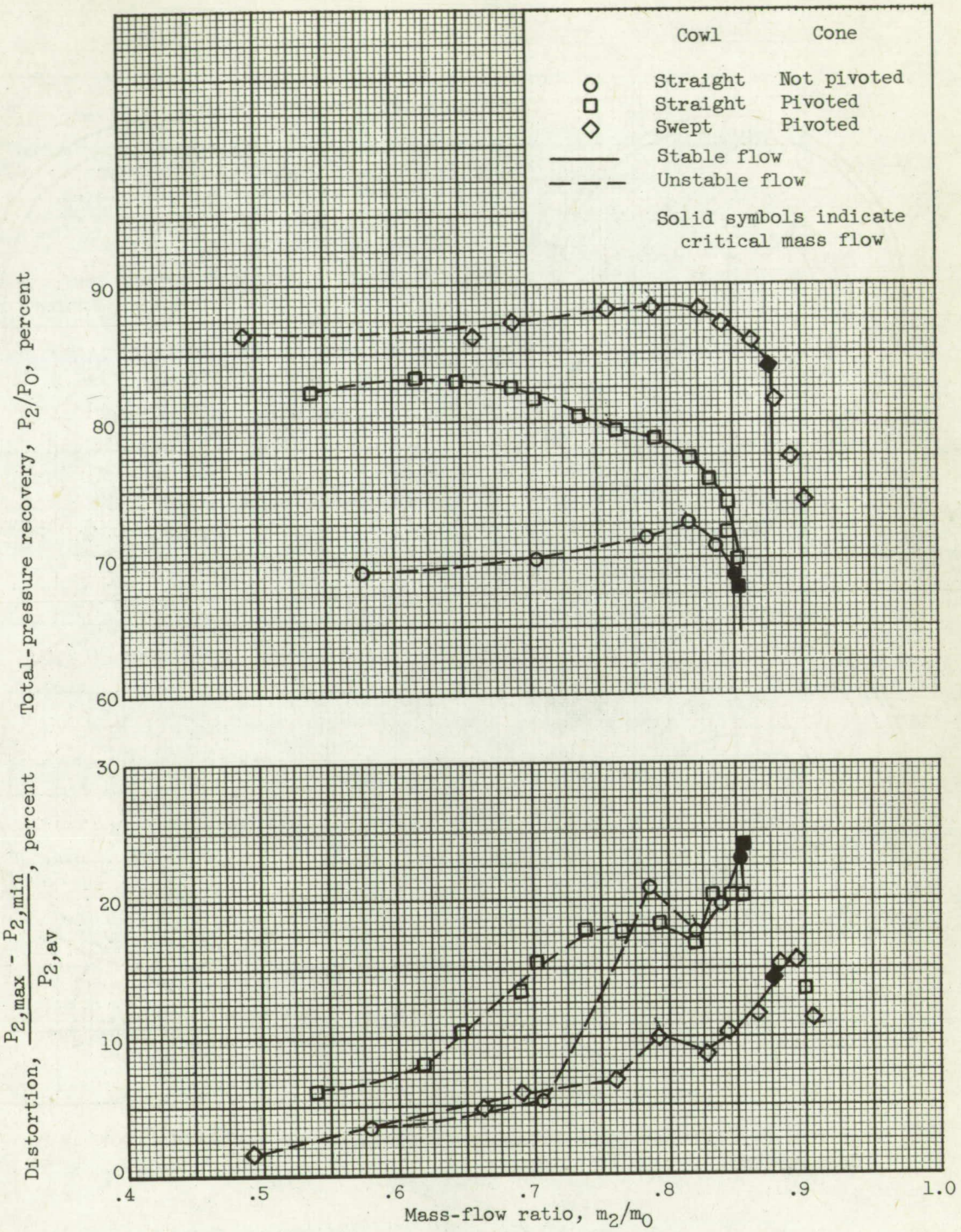
(b) Angle of attack, 6°.

Figure 7. - Continued. Performance curves.



(c) Angle of attack, 10°.

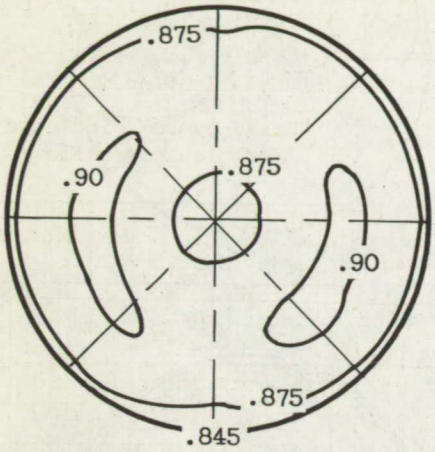
Figure 7. - Continued. Performance curves.



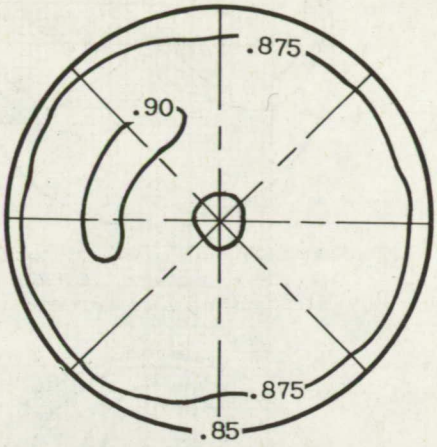
(d) Angle of attack, 14°.

Figure 7. - Concluded. Performance curves.

Straight cowl

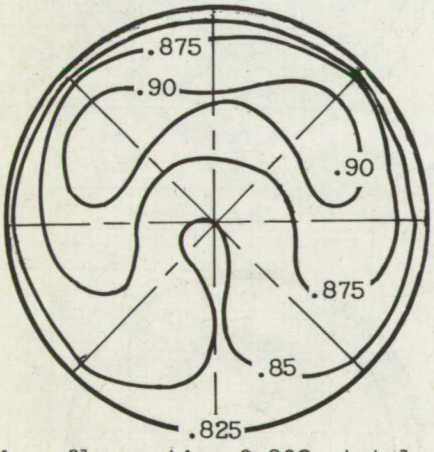


Mass-flow ratio, 0.928; total-pressure recovery, 0.880; distortion, 4 percent.

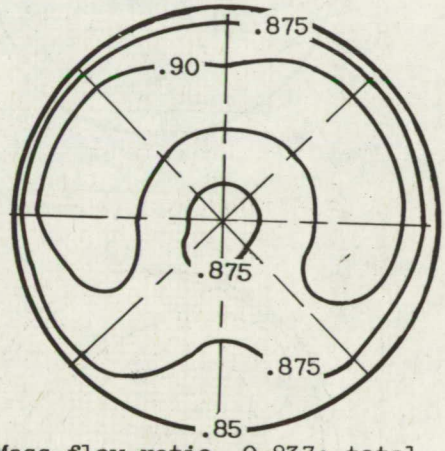


Mass-flow ratio, 0.876; total-pressure recovery, 0.878; distortion, 4.3 percent.

Swept cowl



Mass-flow ratio, 0.902; total-pressure recovery, 0.866: distortion, 9.0 percent.

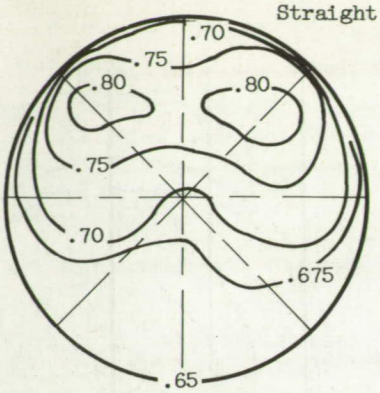


Mass-flow ratio, 0.837; total-pressure recovery, 0.892; distortion, 4.8 percent.

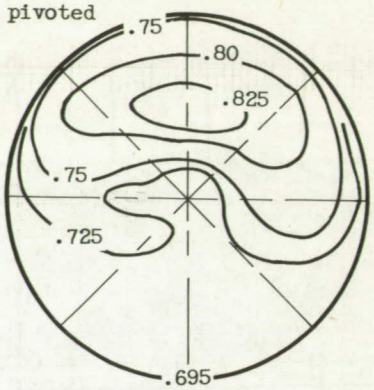
(a) Angle of attack, 0°.

Figure 8. - Diffuser-exit total-pressure-recovery contours (looking downstream).

Straight cowl, cone not pivoted

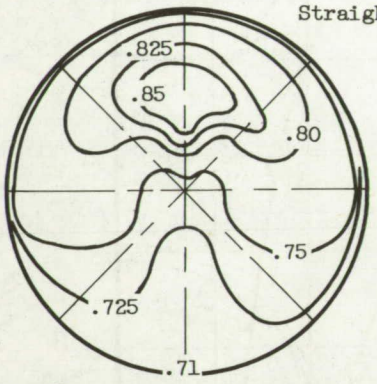


Mass-flow ratio, 0.853; total-pressure recovery, 0.688; distortion, 23.4 percent.

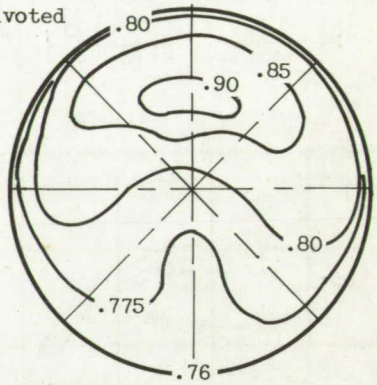


Mass-flow ratio, 0.820; total-pressure recovery, 0.725; distortion, 17.5 percent.

Straight cowl, cone pivoted

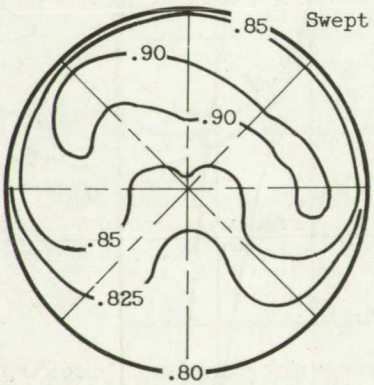


Mass-flow ratio, 0.847; total-pressure recovery, 0.741; distortion, 20.3 percent.

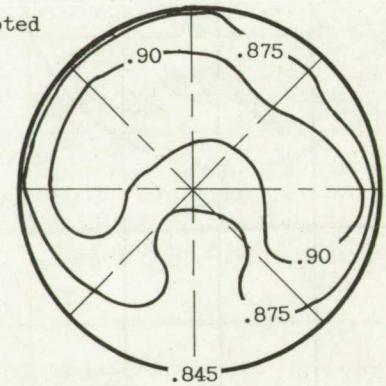


Mass-flow ratio, 0.794; total-pressure recovery, 0.789; distortion, 18.1 percent.

Swept cowl, cone pivoted



Mass-flow ratio, 0.877; total-pressure recovery, 0.84; distortion, 14.2 percent.



Mass-flow ratio, 0.828; total-pressure recovery, 0.88: distortion, 8.8 percent

(b) Angle of attack, 14°.

Figure 8. - Concluded. Diffuser-exit total-pressure-recovery contours (looking downstream).

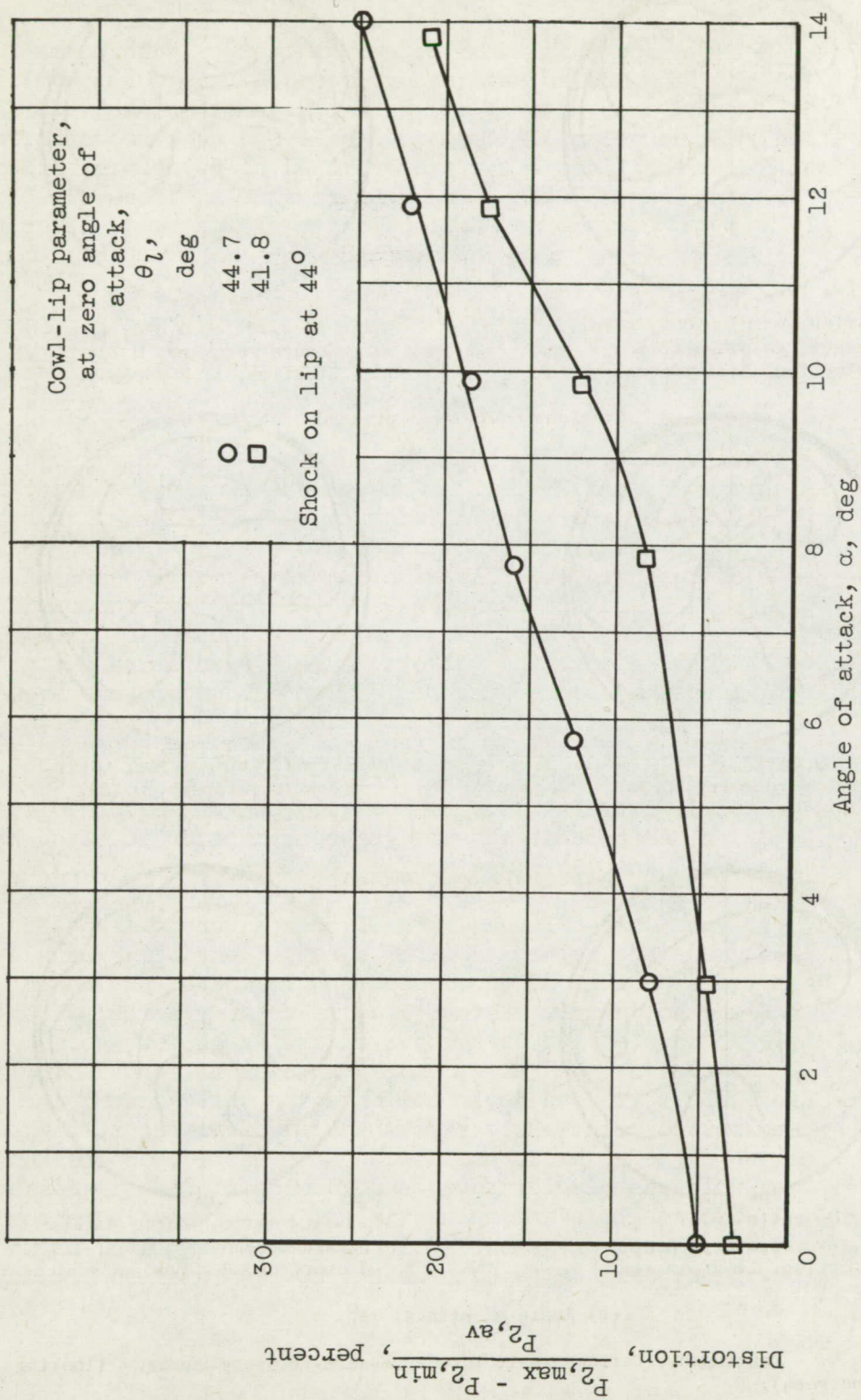


Figure 9. - Effect of cone translation on diffuser-exit distortions of straight-cowl pivoting-cone inlet. Free-stream Mach number, 1.91.